



Why is it imperative to use multicomponent geothermometry in medium/low enthalpy thermal waters? Insights from the Gujarat geothermal region, India

Sitangshu Chatterjee^{1,2} · Parashar Mishra³ · Tirumalesh Keesari^{1,2} · H. J. Pant¹

Received: 16 May 2023 / Accepted: 15 October 2023 / Published online: 7 November 2023
© The Author(s), under exclusive licence to Springer-Verlag GmbH Germany, part of Springer Nature 2023

Abstract

Gujarat area situated in the Cambay rift basin of western India is one of the potential geothermal fields due to its enormous prospects as an oil and gas producing reservoir. The present study attempts to better constrain reservoir temperature by employing the multicomponent fluid geothermometry technique. As the thermal waters in this region undergo extensive mixing with non-thermal saline waters; most of the chemical geothermometers fail to provide the correct estimation of reservoir temperature. For example, the silica and K–Mg geothermometers predict reservoir temperatures below the surface discharge temperatures of the thermal fluids, whereas Na–K and Na–Li geothermometers estimate a wide range of subsurface temperatures (169–226 °C). Na–K–Ca geothermometer computes 158–175 °C as reservoir temperature for thermal waters from Lasundra, Tuwa, and Tulsishyam regions. To solve this ambiguity and to better constrain the reservoir temperature, a multicomponent geothermometry modelling is carried out using GeoT program. Fluid reconstruction is carried out by incorporating the dilution phenomenon. The GeoT modelling of the reconstructed fluids at Dholera region (DH-1) determines the subsurface temperature in the range of 138 ± 7 °C, which matches closely with the values obtained from Na–K–Ca geothermometer (120–126 °C). In the case of thermal waters from Lasundra, Tuwa, and Tulsishyam regions, the GeoT modelling results give a concordant estimation of reservoir temperature in the range of $\sim 165 \pm 10$ °C. This integrated multicomponent method thus emerges as the only viable alternative in providing the correct estimation of reservoir temperature in medium enthalpy geothermal systems.

Keywords India · Thermal waters · Chemical geothermometers · Multicomponent geothermometry · Mixing model

Introduction

The reliable estimation of subsurface reservoir temperature is by far the most important aspect for the development and exploration of any geothermal area. Till date, a wide variety of chemical geothermometers have been utilized to estimate the reservoir temperatures in geothermal systems. Na–K (Arnorsson 1983; Fournier 1979a; Giggenbach et al. 1988;

Nieva and Nieva 1987; Tonani 1980), Na–K–Ca (Fournier and Truesdell 1973), K–Mg (Giggenbach 1988), Na–Li (Kharaka et al. 1982), and silica geothermometers (Fournier 1977) are some of the commonly applied geothermometers in this aspect. Recently, Verma et al. (2008) have developed a ‘SolGeo’ computer program which has incorporated more than 35 geothermometric equations of different solute geothermometers. The application of chemical geothermometers is always based on the tacit assumption of attainment of temperature-dependent fluid–mineral equilibria which is not always valid in all geological settings. Although the chemical geothermometers are found to be most effective in estimating reservoir temperature in high-temperature geothermal systems, they often fail in medium/low enthalpy geothermal systems due to non-attainment of fluid–mineral equilibria (Nitschke et al. 2017, 2018). Interplay of various factors such as mixing between thermal and non-thermal waters, degassing/condensation can also alter the original

✉ Sitangshu Chatterjee
sitanshu@barc.gov.in

¹ Isotope and Radiation Application Division, Bhabha Atomic Research Centre, Mumbai 400085, India

² Homi Bhabha National Institute, Homi Bhabha National Institute, Mumbai, India

³ Geological Survey of India, Northern Region, Lucknow, India

composition of the thermal fluid resulting in deviation from the equilibrium phenomenon. Moreover, the working temperature ranges and the rate of equilibration subsequent to mixing and boiling processes are different for each of the geothermometers. For example, thermal waters in Iceland are found to be in equilibrium with chalcedony geothermometer below 180 °C whereas quartz controls the solubility of the silica above 180 °C. Similarly, Na–K geothermometer is found to work well in high-temperature (180–350 °C) geothermal areas but produces erroneous estimation of subsurface temperature in low-temperature (< 120 °C) geothermal systems due to non-attainment of equilibrium between albite and K-feldspar (Arnórsson 2000). In short, all of the chemical geothermometers have their own advantages and disadvantages and therefore should not be used blindly to estimate the temperature of the subsurface geothermal reservoir. The multicomponent geothermometry method provides a robust means of assessing the subsurface reservoir temperature as it is based on the solid thermodynamic database. In this method, the reservoir temperature is calculated based on the clustering of the saturation indices ($\log(Q/K)$) of reservoir minerals near the zero value (Spycher et al. 2014; Xu et al. 2016). As this method is not dependent on the solubility of the specific minerals, it can be applied in any geological settings provided that the type of reservoir minerals and their detailed chemical analysis is available (Chatterjee et al. 2019).

Apart from these solute geothermometers and multicomponent geothermometry method, there exists several gas geothermometers as well as mixing models which have been used extensively in various geothermal fields across the world to estimate the subsurface reservoir temperature. Gas geothermometers are based on the basic premise that the gas content in geothermal well discharges is controlled by temperature-dependent equilibria with alteration minerals in the reservoir rock and the gas concentrations or gas ratios vary with the temperature of the producing aquifers. A number of gas geothermometers, commonly based on the concentration of a single reactive gas, such as CO_2 , H_2S , H_2 (Arnórsson and Gunnlaugsson 1985), two or more reactive gases such as $\text{CO}_2\text{--H}_2$, $\text{H}_2\text{S--H}_2$ and $\text{H}_2\text{O--H}_2\text{--CO}_2\text{--CO--CH}_4$ (Arnórsson and Gunnlaugsson 1985; Chiodini and Marini 1998) or a ratio of reactive and inert gas such as CO_2/Ar , H_2/Ar and CO_2/N_2 (Giggenbach 1980), have been developed over the last 5 decades to estimate the subsurface temperatures in steam dominated geothermal areas. Recently, the partitioning of the noble gas isotopes has been successfully employed to estimate the subsurface reservoir temperature in the Icelandic geothermal area (Byrne et al. 2021). On the other hand, the mixing models are generally used to estimate the reservoir temperature of the thermal waters that have undergone mixing with non-thermal water or have re-equilibrated in a shallow reservoir (Nicholson 1993, Keesari

et al. 2022). Enthalpy-chloride and enthalpy-silica are the two mixing models commonly applied in various geothermal systems (Fournier 1979b; Truesdell and Fournier 1977).

Gujarat geothermal region, situated in the Cambay rift basin area, hosts nearly 20 thermal springs having surface discharge temperatures varying from 38 to 55 °C. The distinction between thermal and non-thermal waters is made on the basis of the surface discharge temperature. In case of thermal waters, the surface discharge temperature should be consistently above the local mean annual air temperature of that region, whereas in non-thermal waters, surface temperatures remain below than that of local mean annual air temperature (Pentecost et al. 2003) which is 35 °C in study region (Minissale et al. 2003). Therefore, any spring water sample having surface discharge temperature ≥ 35 °C is considered as thermal spring whereas spring water sample having surface discharge temperature less than 35 °C is considered to be non-thermal spring. The present geothermal area is characterized by high heat flow (55–90 mW m^{-2}) and steep geothermal gradient (36–58 °C km^{-1}) (Gupta and Deshpande 2003). The thermal springs in this geothermal region are scattered over several areas like Maktapur, Dholera, Bhadiyad, Lasundra, Tuwa, Lalpur, Tulsishyam, Vankiya, etc. Although previous researchers (Minissale et al. 2003; Shah et al. 2019, 2021) had tried to estimate the reservoir temperature in Gujarat geothermal area by employing various chemical geothermometers, there has been a wide variation in the estimated temperatures. For example, based on the quartz geothermometer, Shah et al. (2019) concluded that the reservoir temperature of Unai geothermal area ranges from 60 to 80 °C. On the other hand, Minisalle et al. (2003) had estimated 120 °C as the reservoir temperature in the Unai area using the same quartz geothermometry. Likewise, in Tulsishyam geothermal area, Minisalle et al. (2003) had estimated 103 °C as the reservoir temperature using silica geothermometry whereas Singh et al. (2018) reported that the reservoir temperature in Tulsishyam area varied from 138 to 207 °C. According to Singh et al. (2018), the quartz geothermometer provided the lower range (138–147 °C) of reservoir temperature in Tulsishyam geothermal area, whereas the upper range (152–207 °C) was calculated from the cation geothermometry. Moreover, in Dholera geothermal area, the base temperature was computed to be ~60 to 80 °C which was slightly higher than the surface discharge temperature (40–47 °C) of the thermal waters in that region. Considering this large variation in reservoir temperature values, a reconnaissance study is carried out to constrain the reservoir temperature both by employing chemical geothermometers as well as multicomponent geothermometry method. This study also focuses on the impact of mixing/dilution processes on the original composition of the thermal fluids and subsequently subsurface reservoir temperature is derived on the basis of the composition of

the reconstructed fluids. Later on, mixing models have also been applied to have the better confidence in the estimated subsurface temperature obtained from multicomponent geothermometry method.

Local geology of the study area

Gujarat state is characterized by its unique geological characteristics and is primarily divided into three major domains, such as Mainland Gujarat, the Saurashtra Peninsula, and the Kachchh Peninsula (Yadav and Sircar 2019). The detailed geological description of the study area can be found in Merh (1995). Broadly, three types of rock formations, i.e., Pre-Champaner Gneissic Complex, Aravalli Supergroup, and Delhi Supergroup, are found in the Mainland Gujarat region. The Pre-Champaner Gneissic Complex (PCGC) represents a suite of rocks comprising gneisses and schists, which form the basement for the Champaner Group (Srikarni and Das 1996). The rocks are represented by micaeous quartzite, quartz-muscovite-biotite gneiss, garnetiferous mica schist, feldspathic biotite gneiss, and granite gneiss (GSI 2017). The Aravalli Supergroup comprises a thick pile of metamorphosed and multiphase deformed clastogenic sediments with some interlayered basic volcanics. Ultramafic and basic rocks generally occur as intrusive in the Aravalli Supergroup. Delhi Supergroup is mainly represented by the Palaeoproterozoic–Mesoproterozoic group of rocks (GSI 2017). The Delhi Supergroup overlies the Aravalli Supergroup with a structural discordance and mainly occurs in the north-eastern part of the Gujarat state (GSI 2001). Most of the thermal waters are found to be confined in the Saurashtra Peninsula, whereas the remaining ones fall in the Mainland Gujarat region. Saurashtra Peninsula is subjected to numerous tectonic events such as inter-continental splitting, rifting, Deccan volcanism, etc. in the past (Mesozoic to Cenozoic) (Singh et al. 2018). Saurashtra Peninsula is comprised of the Precambrian basement overlain by Mesozoic sediments and Deccan lava flows successively (Singh et al. 2018; Rao and Tewari 2005). On the other hand, the Cambay Basin forms the main tectonic structure of the Mainland Gujarat region. The Cambay Basin, formed during the late Cretaceous period, has a graben like structure and is surrounded by numerous major fault systems (Minissale et al. 2003). This Cambay Basin is basically situated in the triple junction area, i.e., in the intersection region of major fault systems like NT (Narmada Tapti) rift system, WC (West Coast) fault system, and Cambay Graben (CG) region. In NT (Narmada Tapti) and CG (Cambay Graben) areas, these fault systems are supposed to extend till mantle depth (~40 km) (Gupta and Deshpande 2003). As a result, the lithosphere underneath the triple junction point is expected to be more ductile, warmer, and thinner compared to other

areas (Pandey and Agrawal 2000). These unique structural characteristics are the main reason for high heat flow values (55–90 mW m⁻²) and high geothermal gradient (temperature gradient 36–58 °C Km⁻¹) in this geothermal region (Gupta and Deshpande 2003). The faults and fractures act as a channel for deeper circulation of the rainwater which emerges as thermal springs after attaining heat in this high heat flow regime. This is the main reason for the occurrence of large number of thermal water manifestations along these well-defined faults and fractures. The geological map along with sample location points is shown in Fig. 1.

Methodology

In this study, 20 thermal water samples and six non-thermal water samples were collected from the Gujarat thermal area. The water sampling campaign was conducted in the month of May, 2016. The field parameters like electrical conductivity (EC), temperature, total dissolved solids (TDS), pH, etc. were measured onsite by a handheld multiparameter probe (HI 9828). One set of acidified samples (concentrated HNO₃, Merck Suprapur[®]) were collected in 250 mL high-density polypropylene (HDPE) bottles for the analysis of cations (Na⁺, K⁺, Ca²⁺, Mg²⁺) and silica, whereas for analysis of anions (Cl⁻, SO₄²⁻), another set of unacidified samples were collected in 250 mL HDPE bottles. The alkalinity of the water samples was determined in the field itself using the standard titrimetric method (APHA 1995). The concentrations of the major cations and anions were analysed using ICP-OES (Inductively coupled plasma-optical emission spectrometry) (Model: ACTIVA, M/S HORIBA Scientific) and ion chromatography (Model: Dionex DX-500) instruments, respectively, whereas lithium and boron concentration were measured using inductively coupled plasma–mass spectrometry (ICP-MS) (Model: Agilent 7800). Sigma-Aldrich makes 1000 ppm standard solutions which were used to prepare the working standards for calibration purposes in both ICP-OES and ICP-MS. External standardisation method was used to prepare the calibration curve and the concentration of unknown samples was analysed by plotting the intensity of the elements of interest against the respective calibration curves. Each standard sample was prepared in Millipore water (18.2 MΩ cm⁻¹) and 1% v/v trace metal grade HNO₃ in such a way that the concentration of the total dissolved solids did not exceed the 0.2 wt% following the measurement protocol by Fernández-Turiel et al. (2000). The detection limit of the ICP-MS instrument for measurement of Li and B is 5 ppb, whereas for other cations and anions, the limit of detection (LOD) was 50 ppb. The precision of the measurement was found to vary between 2 and 5% RSD (relative standard deviation) (Chatterjee et al. 2023). In ion chromatography measurement, the AS

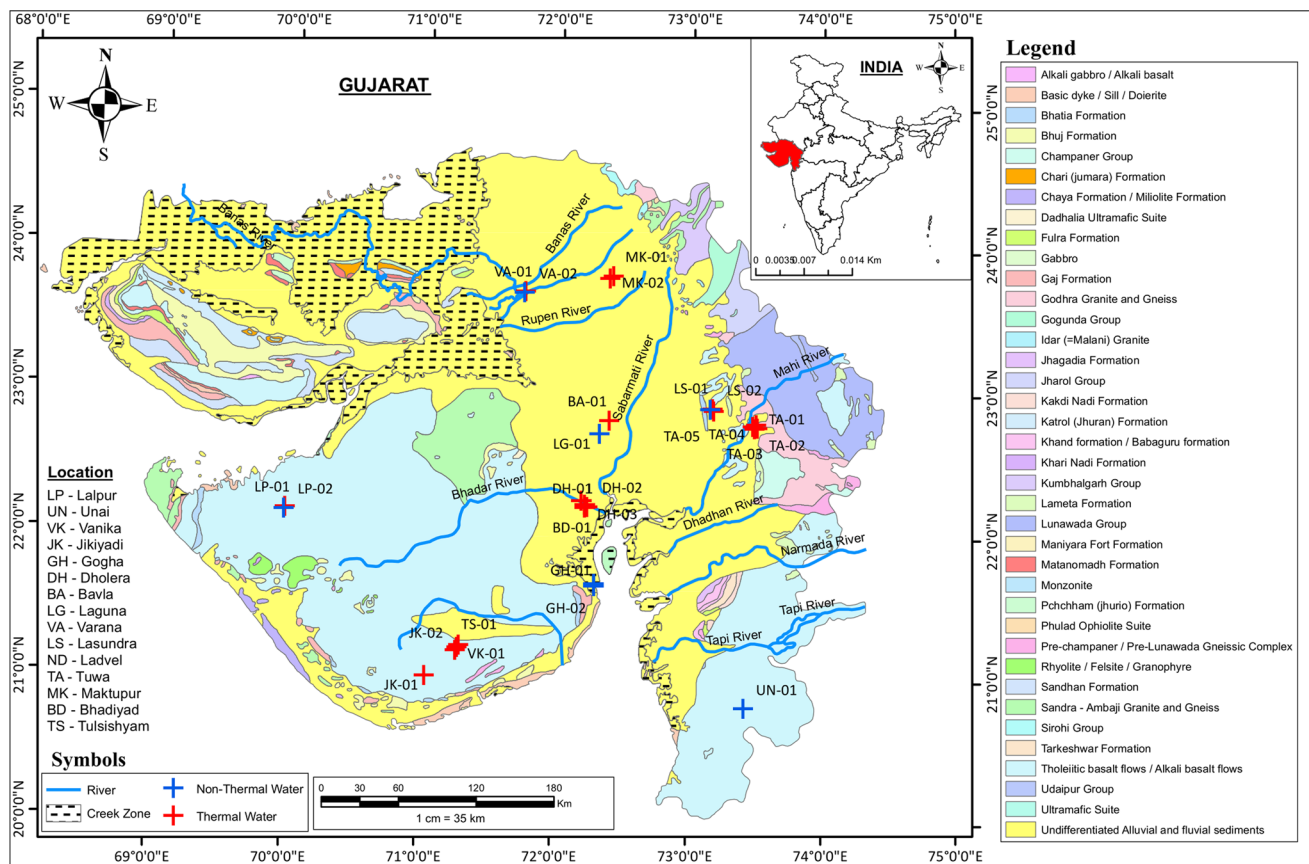


Fig. 1 Geological map along with sample location points in Gujarat geothermal area, India

11 analytical column was used for anion separation. 5–15 mN NaOH solution was used to elute the anions (Keesari et al. 2016). The chemical accuracy was determined by the computing error in charge balance (CBE) (Eq. 1), which was found to be within acceptable limits ($\pm 5\%$)

$$\text{CBE}(\%) = \frac{\text{meq}(\text{cations}) - \text{meq}(\text{anions})}{\text{meq}(\text{cations}) + \text{meq}(\text{anions})} \times 100. \quad (1)$$

Results and discussion

Hydrochemical characteristics

The analysed chemical parameters of all the collected water samples (thermal as well as non-thermal) are given in Table 1. Both the physico-chemical parameters as well as the hydro-chemical parameters of these water samples were recently reported by Chatterjee et al. (2023). Surface emergence temperature of the thermal waters varies from 38 to 55 °C, whereas for non-thermal water samples, the temperature varies from 29 to 33 °C. The pH values of the

collected water samples indicate neutral pH ranging from 7.17 to 8.02. Gaseous emanation was observed in case of the thermal emergences from Tuwa region. The collected gas samples from the present study area were found to contain mostly N_2 (~70 to 90% by volume) followed by CO_2 (~7 to 20% by volume) (Minissale et al. 2003). The thermal waters in the present study area are found to be meteoric in origin (Minissale et al. 2003; Chatterjee et al. 2023). In case of thermal waters, the EC values vary from 525 to 10,860 $\mu\text{S}/\text{cm}$, whereas in case of non-thermal water samples, the EC values range from 290 to 2963 $\mu\text{S}/\text{cm}$. Thermal waters collected from the Lasundra region (LS-02) exhibit highest EC value (10,860 $\mu\text{S}/\text{cm}$), whereas the minimum EC value (525 $\mu\text{S}/\text{cm}$) is reported in the Jikiyadi thermal water (GK-01) of Gujarat state. Among various cations, sodium (Na) concentration is found to be highest (125–1320 ppm) followed by the calcium (Ca) (25–680 ppm), potassium (K) (1–85 ppm), and magnesium (Mg) (5–52 ppm) ions, respectively. Among various anions, chloride (Cl) ion concentration is found to be highest (147–3075 ppm) followed by bicarbonate (HCO_3) (49–378 ppm) and sulphate (SO_4) (16–294 ppm) ions respectively. From the Piper diagram (Fig. 2), it is observed that the thermal water samples can be broadly classified into

Table 1 Chemical parameters of thermal and non-thermal waters (“nd” = not detected, T = thermal, and NT = non-thermal)

Sample ID	Location	Type	Temp (°C)	pH	EC (µS/cm)	TDS (ppm)	Na (ppm)	K (ppm)	Ca (ppm)	Mg (ppm)	SiO ₂ (ppm)	B (ppm)	Li (ppm)	Cl (ppm)	F (ppm)	SO ₄ (ppm)	HCO ₃ (ppm)	Ion balance (%)
GH-01	Gogha	NT	28	7.64	2431	1555	350	13.00	74.0	42.00	14	0.45	0.40	555	0.28	116	361	-3
ND-01	Narmada canal	NT	28	7.93	290	190	8	2.00	28.0	12.00	11	nd	0.20	12	0.18	5	149	-1
LP-02	Lalpur	NT	30	7.52	1394	905	146	2.30	46.0	26.00	21	0.14	0.19	230	0.40	32	200	2
UN-01	Unai	NT	30	7.45	1387	950	175	1.00	110.0	5.00	9	0.13	0.22	300	0.22	48	315	-4
BA-01	Bavla	NT	32	7.71	2963	1895	345	6.00	72.0	58.00	12	0.21	0.30	562	0.60	270	241	-4
LG-01	Laguna	NT	33	7.85	330	215	16	1.00	24.0	16.00	13	0.014	0.23	12	0.30	9	158	2
VA-02	Varana	NT	33	7.57	2134	1450	225	14.00	84.0	52.00	12	0.12	0.50	381	0.30	116	471	-4
VA-01	Varana	T	38	7.4	4198	2730	688	13.00	84.0	52.00	9	0.40	0.51	1160	0.20	164	183	0
GK-01	Jikiyadi	T	40	8.02	525	335	125	1.00	25.0	9.00	19	0.115	0.22	175	0.70	43	90	1
MK-02	Maktupur	T	41	7.84	1168	785	173	2.50	30.0	11.00	23	0.14	0.21	147	2.90	48	375	-5
GK-02	Jikiyadi	T	41	7.68	1329	875	155	2.00	52.0	8.00	17	0.12	0.25	250	0.60	79	55	2
MK-01	Maktupur	T	42	7.75	1248	815	180	3.00	30.0	17.00	11	0.12	0.20	167	2.60	58	378	-4.7
TA-05	Tuwa	T	42	7.22	7104	4615	773	71.00	451.0	7.00	42	0.85	1.75	2025	3.00	231	115	-4
BD-01	Bhadiyad	T	42	7.56	8926	5715	1320	23.00	128.0	67.00	7	1.90	0.90	2650	0.20	48	127	-5
DH-1	Dholera	T	45	7.45	8231	5350	1120	23.00	140.0	45.00	10	1.10	0.80	2212	0.21	28	146	-4
DH-2	Dholera	T	45	7.67	8689	5730	1200	25.00	125.0	45.00	12	1.30	0.70	2350	0.20	16	141	-5
LS-02	Lasundra	T	45	7.29	10,861	7055	1288	85.00	680.0	5.00	49	2.00	3.10	3075	2.70	294	80	-1
TA-04	Tuwa	T	45	7.21	7124	4680	779	67.00	447.0	5.00	26	0.59	1.80	2045	3.00	235	119	-5
VK-01	Vankiya	T	45	7.82	1127	725	119	6.00	50.0	7.00	22	0.12	0.18	200	0.40	75	61	1
DH-3	Dholera	T	47	7.7	7966	5140	1190	27.00	135.0	44.00	8	1.25	0.90	2300	0.26	25	171	-4
LS-01	Lasundra	T	47	7.17	10,416	6770	1180	80.00	632.0	9.00	21	1.50	2.80	2912	2.90	294	63	-2
TA-02	Tuwa	T	48	7.23	7054	4580	780	55.00	440.0	10.00	38	0.70	2.20	2062	3.00	259	125	-5
LP-1	Lalpur	T	48	7.77	1346	870	160	2.00	56.0	11.00	28	0.16	0.20	250	0.30	98	100	0
TA-01	Tuwa	T	53	7.21	6996	4540	781	50.00	425.0	6.00	50	1.80	1.96	2075	3.00	248	119	-7
TS-01	Tul-sishyam	T	54	7.36	1937	1235	215	18.00	120.0	14.00	53	0.45	0.60	470	5.00	100	102	-1
TA-03	Tuwa	T	55	7.45	6898	4495	788	65.00	424.0	5.00	60	0.68	2.40	2050	3.00	242	110	-4.5

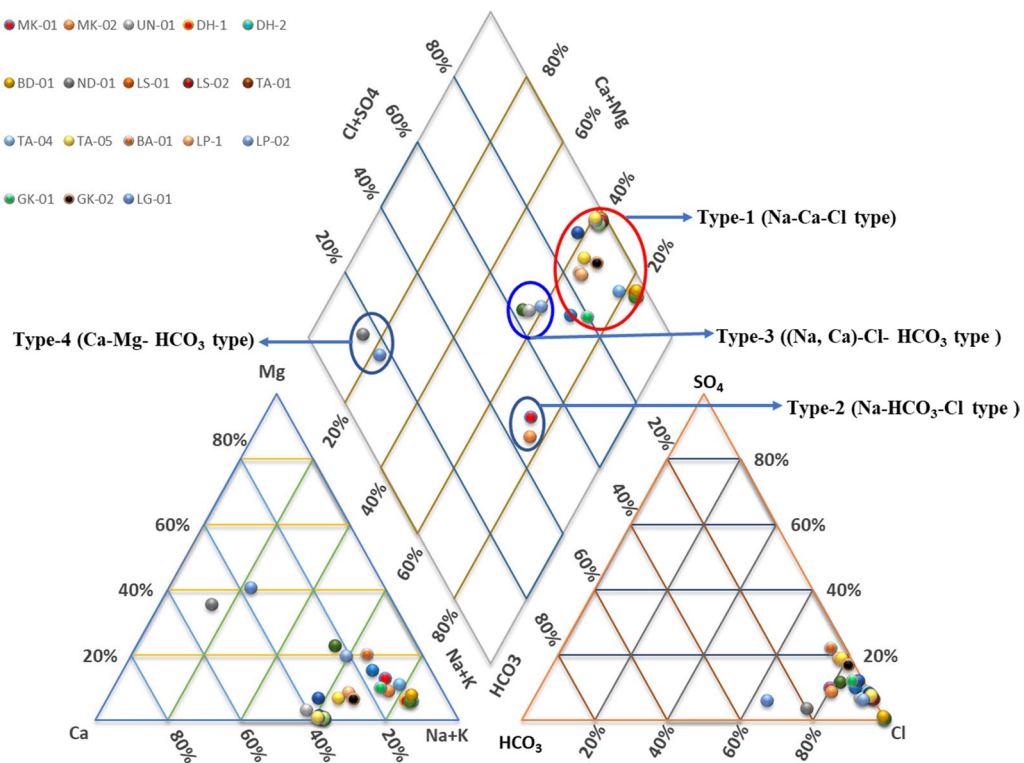


Fig. 2 Piper diagram of the water samples collected from the study area

two major geochemical types: (1) Na–Ca–Cl type (GK-2; LP-1, LS-1, 2; TA-1,2,3,4,5; VK-1; TS-1, BD-1; DH-1,2,3; GK-1; VA-1) (Type-1), (2) Na–HCO₃–Cl type (MK-1, 2) (Type-2) whereas the non-thermal water samples can be grouped into two distinct categories: (3) Mixed cation (Na, Ca)–Cl–HCO₃ type (LP-2; UN-1; VA-2; GH-1) (Type-3) and (4) Ca–Mg–HCO₃ type (ND-1 and LG-1) (Type-4). Thermal water samples from Bhadiyad (BD-1), Dholera (DH-1, 2, 3), Lasundra (LS-1, 2) and Tuwa (TA-1,2,3,4,5) fall near to the chloride corner in the Cl–SO₄–HCO₃ ternary diagram (Fig. 3) which indicates that they are mature in nature. The thermal water samples from Maktupur region (MK-1 and MK-2) fall in the peripheral water region which implies that their chemical signature closely matches with the non-thermal water samples. Rest of the thermal waters (i.e., VA-1; TS-1; GK-1, 2; LP-1; VK-1) fall in between the mature and peripheral water regions. None of the thermal waters in the present study area resembles the chemical composition of the steam-heated local groundwater or the volcanic water samples.

Apart from the major ions, boron and lithium are the two other important trace elements which are often investigated in the geothermal systems. Being fluid mobile elements, the distributions of the chloride, boron, and lithium in geothermal systems have been used to trace elemental sources and interpret various subsurface processes (Legros

et al. 2016; Lopez et al. 1993; Trumbull and Slack 2018). For example, chloride-to-boron (Cl/B) values are often used to trace the type of reservoir rock through which thermal water interacts as well as to assess the mixing phenomenon between the thermal and non-thermal waters in the up-flow zones of geothermal systems (Goff et al. 1988; Arnórsson and Andrésdóttir 1995; Giggenbach 1995). In the present study area, for non-thermal water samples, the boron concentrations are found to vary from 0.014 ppm (14 ppb) (LG-01) to 0.45 ppm (450 ppb) (GH-01), whereas for thermal waters, the boron concentrations range from 0.12 (120 ppb) (MK-01) to 2 ppm (2000 ppb) (LS-02). Similarly, for non-thermal water samples, the lithium concentrations are found to vary from 0.19 (190 ppb) (LP-02) to 0.50 ppm (500 ppb) (VA-02), whereas for thermal water samples, the lithium concentrations range from 0.18 (180 ppb) to 3.1 ppm (3100 ppb) (LS-02). The higher concentration of boron and lithium ions in the thermal waters can be attributable to the mixing with the paleo-seawater entrapped in the formations (Chatterjee et al. 2023). The near linear correlation ($R^2 = 0.83$) (Fig. 4a) between the chloride and boron concentrations of the thermal and non-thermal waters in the present study area clearly points out to the mixing phenomenon in the up-flow zones. Similar type of linear relationship is observed between the chloride and lithium ion (Fig. 4b) concentrations of the

Fig. 3 Cl–SO₄–HCO₃ ternary diagram of thermal water samples

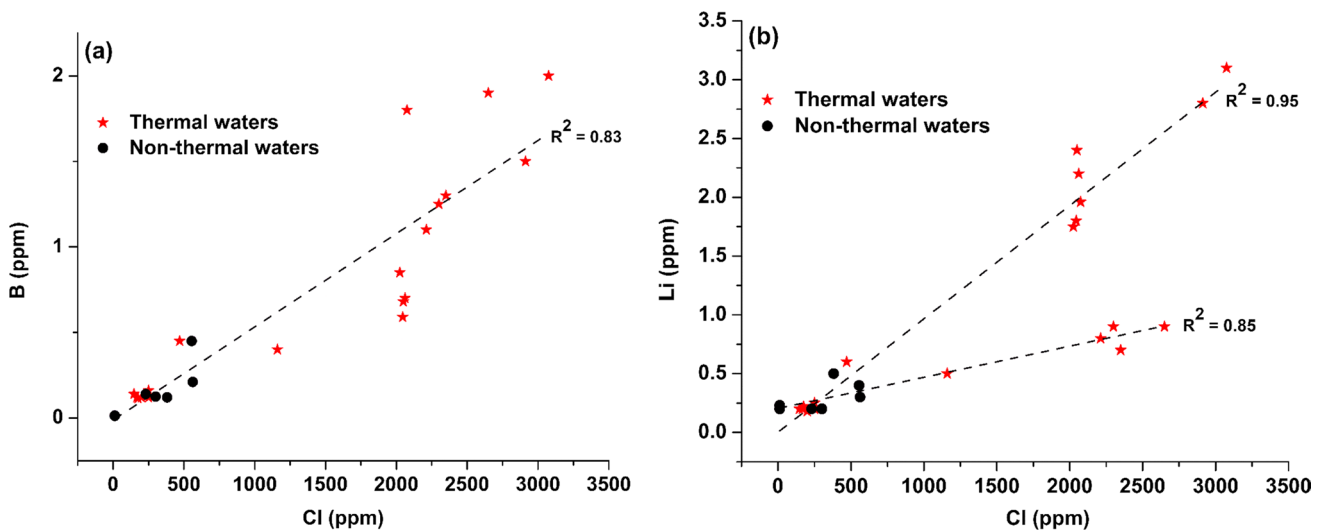
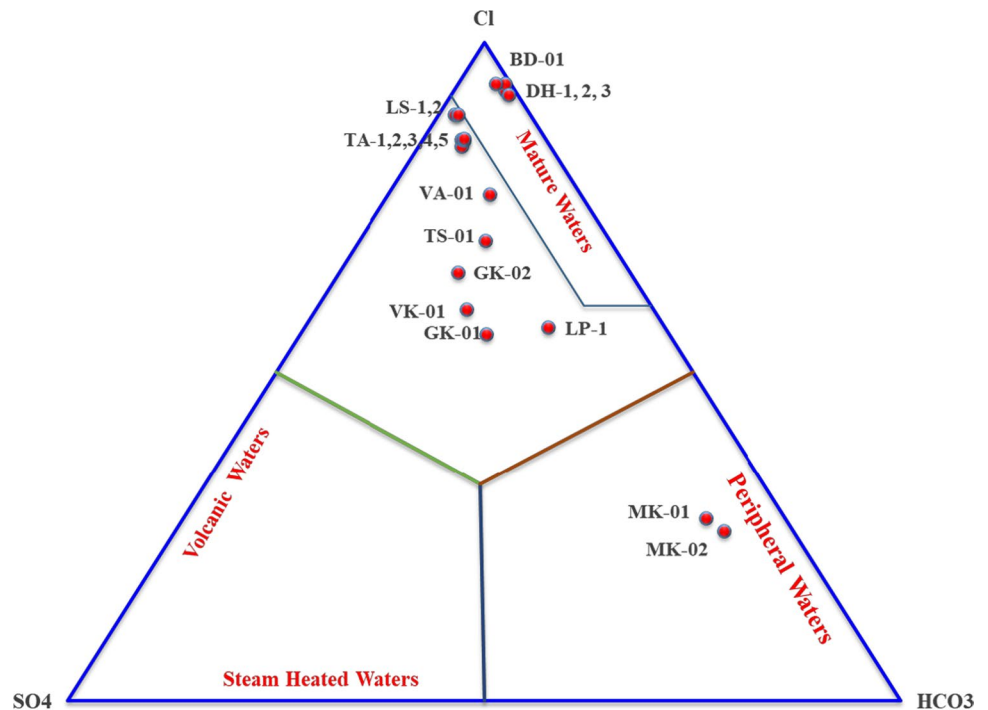


Fig. 4 Graphical plot between **a** boron vs. chloride and **b** lithium vs. chloride to elucidate the mixing process

thermal and non-thermal waters which also signifies the mixing between thermal and non-thermal water samples.

Estimation of reservoir temperature

Chemical geothermometers

The computed reservoir temperatures of the present study area obtained by applying the silica and cation geothermometers are given in Table 2.

Silica geothermometer Silica has various polymorphs in nature, such as quartz, chalcedony, amorphous silica, cristobalite, tridymite, etc. Among all the silica polymorphs, only quartz and chalcedony phases assume significance in geothermal studies. Quartz geothermometer can be further classified into two types: (1) conductive quartz geothermometer (considering no steam loss while coming to the surface) and (2) adiabatic quartz geothermometer (which accounts for the maximum steam loss phenomenon while coming to the surface). The reservoir temperature estimated from the con-

Table 2 Estimated reservoir temperatures (°C) using chemical geothermometers

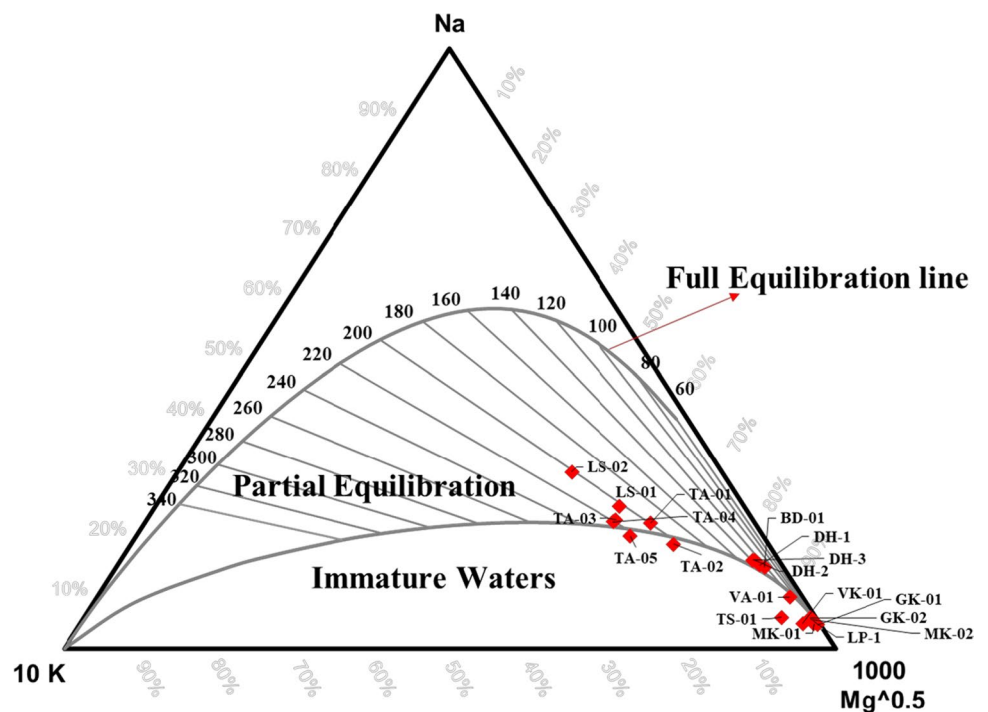
Sample ID	Chalcedony (conductive) Arnoors-son (1983)	Quartz (conduc-tive) Fournier (1977)	Quartz (Abi-atic) Fournier (1977)	K/Mg Giggensbach (1988)	Na-K-Ca Fournier and Truesdell (1973)	Na/Li Kah-raka et al. (1982)	Na/K Fournier (1979a)	Na/K Tonani (1980)	Na/K Arnorsson (1983)	Na/K Nieva and Nieva (1987)	Na/K Giggensbach (1988)
VA-01	3	34	44	55	114	133	106	80	70	96	127
MK-1	10	41	50	37	58	153	100	72	64	90	121
MK-2	37	69	74	38	58	155	102	64	56	83	114
DH-1	7	38	47	69	120	132	111	85	75	100	131
DH-2	13	44	53	71	23	123	111	86	76	101	132
DH-3	-1	30	41	73	126	135	116	91	81	105	136
BD-1	-5	25	37	65	117	130	102	75	66	92	123
LS-1	33	66	71	124	164	194	186	180	158	173	203
LS-2	71	101	102	136	163	195	184	177	156	171	201
TA-1	72	102	103	116	168	197	182	174	154	169	199
TA-2	59	90	92	111	162	205	189	184	162	176	206
TA-3	81	111	110	127	170	209	201	201	176	188	217
TA-4	42	74	78	128	172	192	204	205	180	191	221
TA-5	63	94	96	124	175	191	210	213	186	197	226
LP-1	45	77	81	33	35	159	86	56	49	76	107
TS-1	75	105	105	77	160	204	202	202	178	189	219
VK-1	35	67	72	60	134	169	165	152	134	153	183
GK-1	29	62	67	23	29	177	67	34	29	57	88
GK-2	25	57	64	36	36	172	88	58	51	78	109

ductive quartz geothermometer (Fournier 1977) ranges from 34 to 105 °C, whereas the adiabatic quartz geothermometer (Fournier 1977) computes the subsurface temperature in the range of 37–110 °C. It can be easily observed that in several geothermal areas, such as Varana (VA-1), Maktupur (MK-1), Dholera (DH-1, 2 and 3), Bhadiyad (BD-1) region, the estimated subsurface reservoir temperatures using the conductive quartz geothermometer are below the surface discharge temperatures of the thermal fluids. Therefore, quartz geothermometer is unreliable one in the present geothermal area. In other geothermal areas, such as Lasundra (LS-1, 2), Tuwa (TA-1,2,3,4,5), and Tulsishyam (TS-1), the quartz geothermometer provides the minimum estimation of the subsurface reservoir temperature. This can be attributed to the extensive dilution of thermal waters with non-thermal waters (Minissale et al. 2003), and as a result, the silica concentration decreases significantly resulting underestimation of the reservoir temperature. On the other hand, the chalcidony geothermometer computes still lower estimation of reservoir temperature, and in some areas (BD-1, DH-3), it even gives negative reservoir temperature (– 5 and – 1 °C) which is practically impossible. Therefore, the chalcidony geothermometer is also ineffective in this medium enthalpy geothermal field.

Cation geothermometers Among various cation geothermometers, the most widely used geothermometers are: Na–K geothermometers (Arnorsson 1983; Fournier 1979a; Giggenbach 1988; Nieva and Nieva 1987; Tonani 1980), Na–K–Ca geothermometer (Fournier and Truesdell 1973),

K–Mg geothermometer (Giggenbach 1988), and Na–Li (Kharaka et al. 1982). Figure 5 represents the Giggenbach’s (1988) Na–K–Mg geoindicator triangular diagram which is basically used to assess the extent of attainment of equilibrium during the rock–water interaction. Depending on the extent of equilibration, the Na–K–Mg ternary diagram is generally divided into three regions: immature region, partially mature region, and full equilibration region. It is observed from Fig. 5 that the thermal waters from Maktupur (MK-1 and MK-2), Varana (VA-1), Jikiyadi (GK-1,2), Tulsishyam (TS-1), and Vankiya (VK-1) region fall in the ‘immature region’ which implies that the application of Na–K geothermometer would not be appropriate in these areas. Thermal water samples from Dholera (DH-1, 2 and 3) and Bhadiyad (BD-1) area fall near the intersection curve of ‘immature region’ and ‘partial equilibration region’ indicating that the Na–K geothermometer can be applied with careful consideration. On the other hand, thermal water samples from Lasundra (LS-1, 2) and Tuwa (TA-1, 3, 4) fall on the ‘partial equilibration region’ implying that the cation geothermometer can be applied with some confidence for these samples. The Lasundra (LS-1, 2) samples fall on the line intersecting the ‘full equilibration line’ at 200 °C, whereas the thermal waters from Tuwa (TA-1,2,3,4,5) area show the average subsurface temperature in the range of 200–220 °C which need to be corroborated by other geothermometric methods. In case of thermal waters from Lasundra (LS-1, 2) and Tuwa (TA-1,2,3,4,5) region, various Na–K geothermometers as developed by Fournier (1979a), Giggenbach (1988), Tonani (1980), and Nieva and Nieva (1987) also esti-

Fig. 5 Na–K–Mg ternary diagram (Giggenbach 1988) of thermal water samples



mate the subsurface temperature in the range of 169–226 °C (Table 2) which matches closely with the values obtained from the Na–K–Mg ternary diagram. However, Na–K geothermometer as developed by Arnorsson (1983) estimates somewhat lower reservoir temperature (154–186 °C) in Lasundra and Tuwa region.

From the above discussion, it is quite obvious that although Na–K geothermometer is found to be somewhat suitable only in Lasundra and Tuwa region still, it is not able to provide concordant estimation of subsurface temperature in other areas.

The Na–K–Ca geothermometer, originally proposed by Fournier and Truesdell (1973), has been applied successfully in estimating the reservoir temperatures for thermal waters having high concentration of calcium ions (Nicholson 1993). In low-temperature and non-equilibrated thermal water systems, the Na–K–Ca geothermometer is generally preferred, because it does not give misleading (abnormally high and/or low) reservoir temperature estimation as obtained from applying silica and Na–K geothermometers (Arnorsson 2000) which is exemplified in case of the thermal waters from Varana (VA-1), Dholera (DH-1, 2 and 3), Bhadiyad (BD-1), and Vankiya (VK-1) regions. In these regions, the Na–K–Ca geothermometer computes reservoir temperature varying from 114 to 134 °C which seems more probable and also closely matches with the values obtained from applying the Na–K geothermometers (Fournier 1979a; Giggenbach 1988). From the previous discussions (“Silica geothermometer”), it is observed that the quartz geothermometer fails to predict the subsurface reservoir temperatures in Varana (VA-1), Dholera (DH-1, 2 and 3), and Bhadiyad (BD-1) regions as the estimated temperatures fall below the surface discharge temperatures of the thermal fluids. In case of thermal waters from Lasundra (LS-1, 2), Tuwa (TA-1, 2, 3, 4, 5), and Tulsishyam (TS-1) region, the estimated subsurface temperature from Na–K–Ca geothermometer ranges from 158 to 175 °C. However, the Na–K–Ca geothermometer fails to estimate the subsurface temperature in thermal waters from Maktupur (MK-1, 2), Jikiyadi (JK-1, 2), and Lalpur (LP-1) region as the estimated subsurface temperatures (29–58 °C) fall below the surface discharge temperature of thermal waters (40–42 °C).

The other cation geothermometer mainly, K–Mg, is not suitable in the present geothermal area as the Mg concentrations in most of the thermal waters are found to be high (11–67 ppm) due to the near surface mixing with non-thermal waters (Nicholson 1993). This is confirmed from the estimated reservoir temperature in Maktupur (MK-1 and MK-1) and Lalpur (LP-1) regions where estimated reservoir temperature is lower than the surface discharge temperature.

The Na–Li geothermometer constitutes another important cation geothermometer which has found widespread use in the case of hot saline waters from oil-field, sedimentary

basins, etc. For saline fluids, Na–Li geothermometer can be considered very useful tool considering the low Li reactivity during the ascent the geothermal fluid up to the surface. The Na–Li geothermometric equation developed by Kahraka et al. (1982) is used to estimate the subsurface temperature of brines in sedimentary basins (Sanjuan et al. 2014). In Lasundra (LS-1, 2), Tuwa (TA-1,2,3,4,5), and Tulsishyam (TS-1) region (where EC ranges from 6898 to 10,861 $\mu\text{S}/\text{cm}$), the Na–Li geothermometer estimates reservoir temperature in the range of 190–204 °C which matches with that of the Na–K geothermometer values (Fournier 1979a; Giggenbach 1988). Similarly, in case of thermal waters from Dholera region (EC ranges from 7966 to 8689 $\mu\text{S}/\text{cm}$), the calculated reservoir temperature from Na–Li geothermometer matches excellently with the values obtained from Na–K–Ca geothermometer and Na–K geothermometer (Giggenbach 1988).

Multicomponent fluid geothermometry

From the preceding discussion, it has been observed that the both the silica geothermometer as well as cation geothermometers fail to provide unequivocal estimation of reservoir temperature in the study area. As a result, multicomponent fluid geothermometry method has been employed which has emerged as a useful tool to predict the reservoir temperature particularly in the medium and/or low enthalpy geothermal areas (Reed and Spycher 1984; Pang and Reed 1998; Spycher et al. 2014; Hou et al. 2019; Olguín-Martínez et al. 2022). The impact of various subsurface processes, such as dilution and degassing, can also be accounted in this multicomponent geothermometry method. These subsurface processes alter the original chemical composition resulting the wrong estimation in the reservoir temperature. A stand-alone computer program, GeoT, is employed to perform the multicomponent geothermometry calculation. The thermodynamic database SOLTHERM.H06 is used in this GeoT program to compute both the ion activity product (Q) and the thermodynamic equilibrium constant (K) of different minerals at different temperatures. The detailed procedure of this method can be found in Spycher et al. (2014). In this study, calcite, aragonite, quartz, kerolite, diopside, anthophyllite, tremolite, phlogopite, cummingtonite, and brucite are chosen as ten main clustering minerals based on the saturation study of minerals by Minissale et al. (2003).

Initial analysis of the thermal waters One thermal water sample each from Dholera (DH-1), Lasundra (LS-1), Tuwa (TA-3), and Tulsishyam (TS-1) regions has been chosen for further investigation. The multicomponent geothermometry method, applied on the original chemical composition (without accounting dilution and parameter optimization) of the thermal waters from Dholera (DH-1), Lasundra (LS-1),

Tuwa (TA-3), and Tulshishaym (TS-1) regions, has computed the subsurface temperatures in the range of 58–80 °C (Fig. 6a–d) which is even lower than the temperature estimated from the silica geothermometers (~ 110 °C). This suggests the alteration of original chemical composition of the thermal fluids due to the presence of various secondary processes.

Deep fluid reconstruction The stand-alone GeoT computer program is found to be very effective in optimizing some of the unknown and/or poorly constrained parameters. In the present study area, the effect of mixing/dilution on the original composition of the thermal waters has been corrected using the dilution factor ('cfact') in the GeoT program. The value of the dilution factor ('cfact') varies depending on the extent of mixing with the non-thermal waters and the GeoT program will numerically optimize the dilution factor ('cfact') till a good clustering is achieved.

Now, when the Dholera thermal water (DH-1) is run again by numerically optimizing the dilution factor (cfact = 0.4) parameter, a very good clustering of selected minerals is observed at the reservoir temperature of 138 ± 7 °C (Fig. 7a).

This temperature estimation closely matches with the values obtained from Na–K–Ca geothermometer (120–126 °C) as well as Na–K geothermometer (131–136 °C) (Giggenbach 1988). GeoT program also computes different statistical parameters like median (RMED), mean (MEAN), standard deviation (SDEV), and root-mean square error (RMSE) of saturation indices and the temperatures at which these statistical parameters attain minimum value (T_{RMED} , T_{MEAN} , T_{SDEV} , and T_{RMSE}). For a perfectly clustered system, T_{RMED} , T_{MEAN} , T_{SDEV} , and T_{RMSE} should be identical, and this temperature reflects the computed reservoir temperature. Figure 7b shows that in case of DH-1 sample, all the statistical parameters like RMED, MEAN, SDEV, and RMSE attain the minimum value ~ 138 °C which can be considered as the most probable subsurface reservoir temperature.

In case of Lasundra thermal water (LS-1), the parameter optimization (cfact = 0.3) of the dilution effect has resulted in clustering of minerals around 160 ± 10 °C which can be considered as the most probable reservoir temperature (Fig. 7c). In case of LS-1 sample, all the statistical parameters like RMED, MEAN, SDEV, and RMSE attain the minimum value at ~ 160 °C (Fig. 7d) which denotes

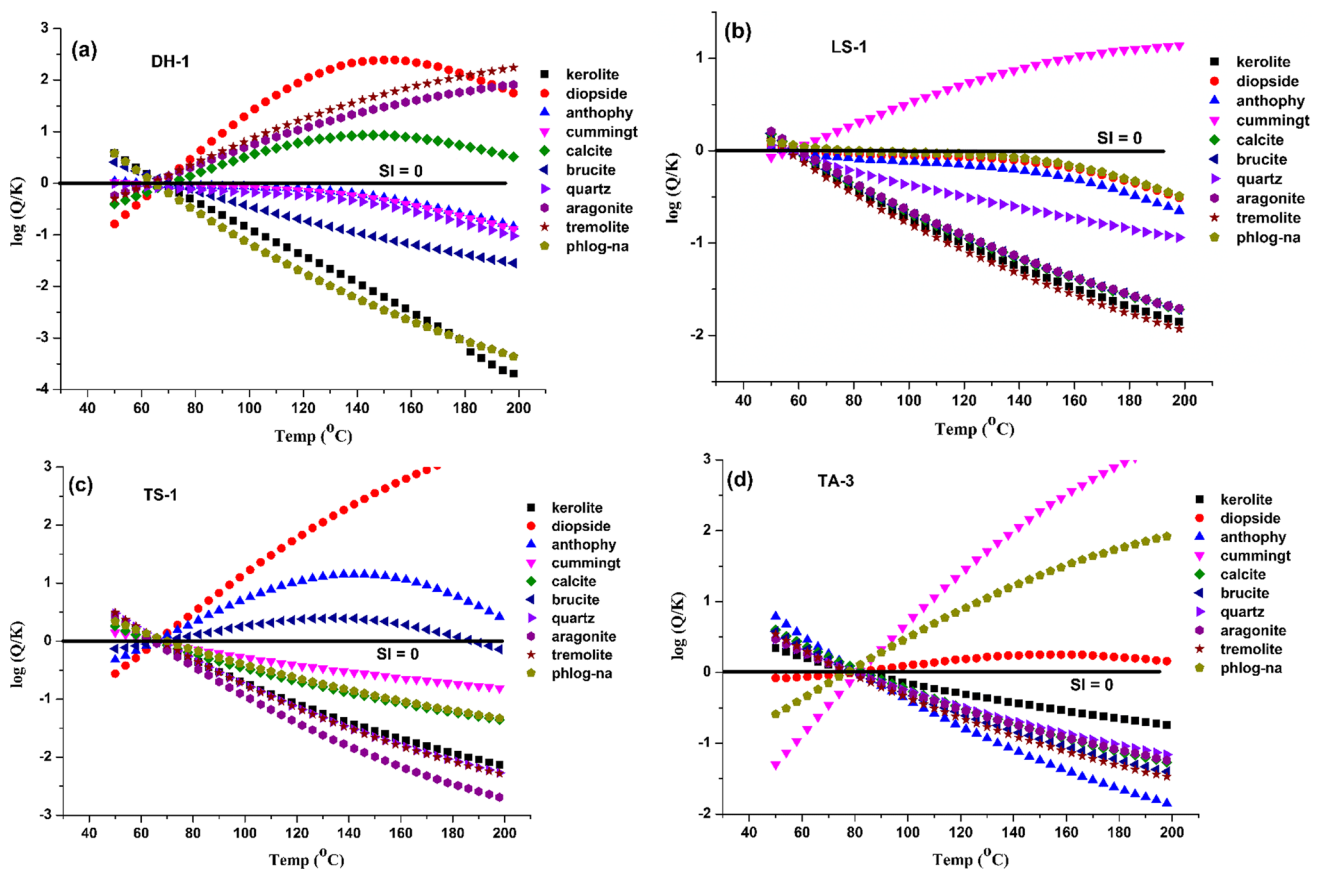


Fig. 6 Variation of mineral saturation indices ($\log(Q/K)$) vs. temperature for uncorrected fluid compositions of **a** Dholera (DH-1), **b** Lasundra (LS-1), **c** Tulsishyam (TS-1), and **d** Tuwa (TA-3)

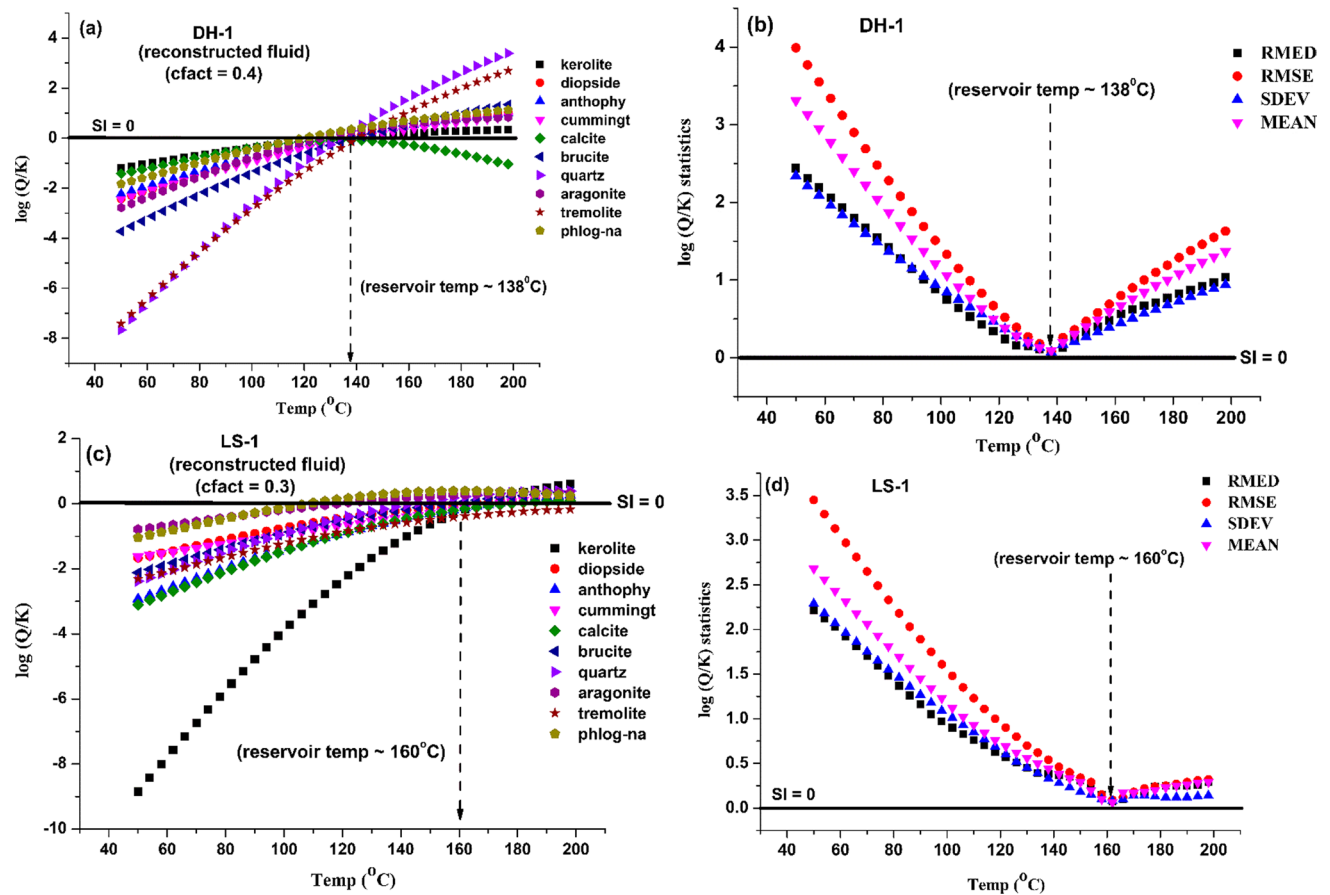


Fig. 7 Estimation of reservoir temperature of reconstructed fluids from Dholera (DH-1) region **a** minerals vs. temperature plot, **b** statistical parameters vs. temperature plot and Lasundra (LS-1) region, **c** minerals vs. temperature plot, and **d** statistical parameters vs. temperature plot

the probable subsurface reservoir temperature. In this case, although the temperature estimation from the multicomponent geothermometry method matches with the Na–K–Ca geothermometer values (163–164 °C), they are found to be significantly lower than what is predicted from Na–K (Giggenbach 1988) and Na–Li (Kahraka et al. 1982) geothermometers.

In case of Tuwa thermal water (TA-3) sample (TA-3 shows the highest surface discharge temperature), the deep fluid reconstruction was carried out by employing both the dilution factor ($c_{\text{fact}}=0.10$) and the steam fraction factor ($stwf=0.15$). The steam fraction ($stwf$) factor is used to add the gas back into the deep fluid which has lost due to boiling. The steam fraction ($stwf$) factor is used in the TA-3 sample as gaseous emanations were observed during sampling. The incorporation of both the ' c_{fact} ' and the ' $stwf$ ' of the Tuwa thermal water (TA-3) sample (TA-3) has resulted the clustering of minerals in the range of 166 ± 12 °C (Fig. 8a). At this temperature range, $\log(Q/K)$ values of all the statistical parameters such as mean (MEAN), median (RMED), root-mean-square error (RMSE), and standard deviation (SDEV) also attain minimum value thereby indicating the

probable reservoir temperature in the Tuwa region (Fig. 8b). Similarly, deep fluid reconstruction method applied in the Tulshishaym (TS-1) thermal water ($c_{\text{fact}}=0.15$) shows that the reservoir temperature is 168 ± 8 °C (Fig. 8c, d) which is quite similar to the subsurface temperature obtained from Lasundra and Tuwa region.

We have also carried out GeoT modelling studies of the thermal waters from Dholera and Lasundra area using the chemical composition as reported by the Minissale et al. (2003). After fluid reconstruction study, the estimated reservoir temperature for Dholera sample is found to be ~ 124 °C (supplementary file, Fig. S1) which is similar to the temperature estimated in this study (138 ± 7 °C). For Lasundra thermal water, the GeoT modelling of the reconstructed fluid (Minissale et al. 2003) computes ~ 150 °C (supplementary file, Fig. S2) as reservoir temperature which is again similar to the values estimated in the present study (165 ± 10 °C). In case of Tulsishyam thermal water, Minissale et al. (2003) reported silica concentration as 151 ppm which gives quartz geothermometer value of ~ 162 °C matching closely with the temperature estimated in the present study. Therefore, based on the above discussions, it can be concluded that

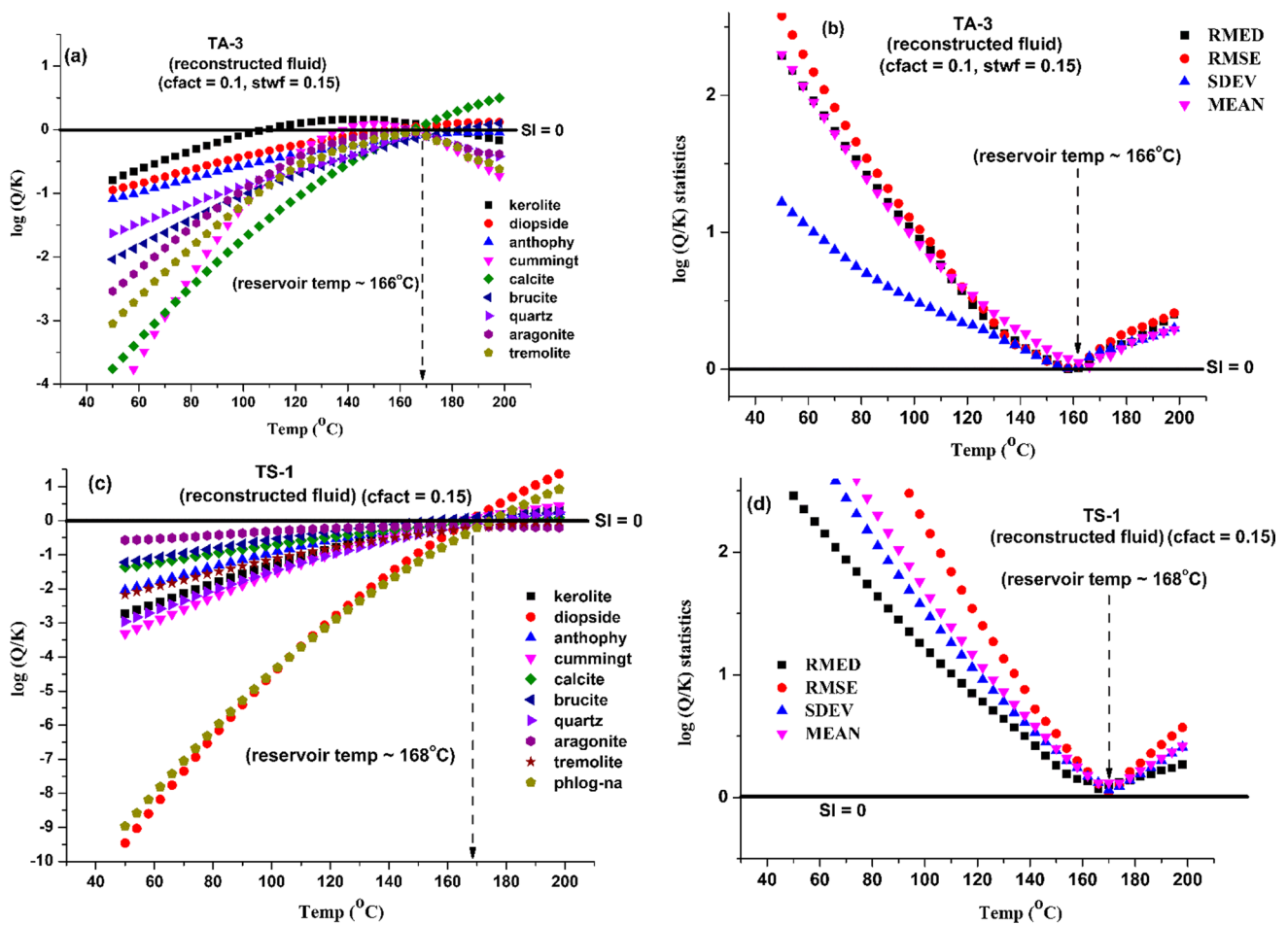


Fig. 8 Estimation of reservoir temperature of reconstructed fluids from Tuwa (TA-3) region, **a** minerals vs. temperature plot, **b** statistical parameters vs. temperature plot and Tulsishyam (TS-1) region, **c** minerals vs. temperature plot, and **d** statistical parameters vs. temperature plot

the multicomponent geothermometry method gives similar temperature estimation in both the occasions.

Mixing models

To further corroborate the multicomponent geothermometry results, mixing models have been used to estimate the reservoir temperature in the Gujarat geothermal region. The enthalpy–silica and the enthalpy–chloride mixing models are normally used to estimate subsurface temperature of the mixed thermal waters (Truesdell and Fournier 1977; Fournier 1979b).

Enthalpy–silica mixing model

In the enthalpy–silica mixing model, the enthalpy is used as an axis rather than temperature, because combined heat content (enthalpy) of the two waters remains conserved upon mixing, whereas the combined temperatures are not (Fournier 1989). In this mixing model, the silica

concentrations of the samples were plotted against their corresponding onsite enthalpies. The enthalpy values were determined using the steam tables of Keenan et al. (1969). For the application of this model, two end-member fluids are generally considered: dug well samples (representing non-thermal groundwater sample) as one end member and the thermal water samples as the other end member. The subsurface temperature of the geothermal reservoir can then be obtained by two different methods. In the first method (Fig. 9a), it is assumed that no steam or heat loss takes place before mixing. A line joining the composition of local ground waters (dug well samples) and thermal water samples intersects the no steam loss curve at point A. A vertical line from point A intersects the enthalpy axis at point B, which represents the enthalpy of the parent geothermal water before mixing. In the present case, the subsurface temperature [after converting enthalpy to temperature using the steam tables of Keenan et al. (1969)] turns out to be ~ 211 °C which is abnormally high. According to Fournier and Truesdell (1973), this type of situation arises when

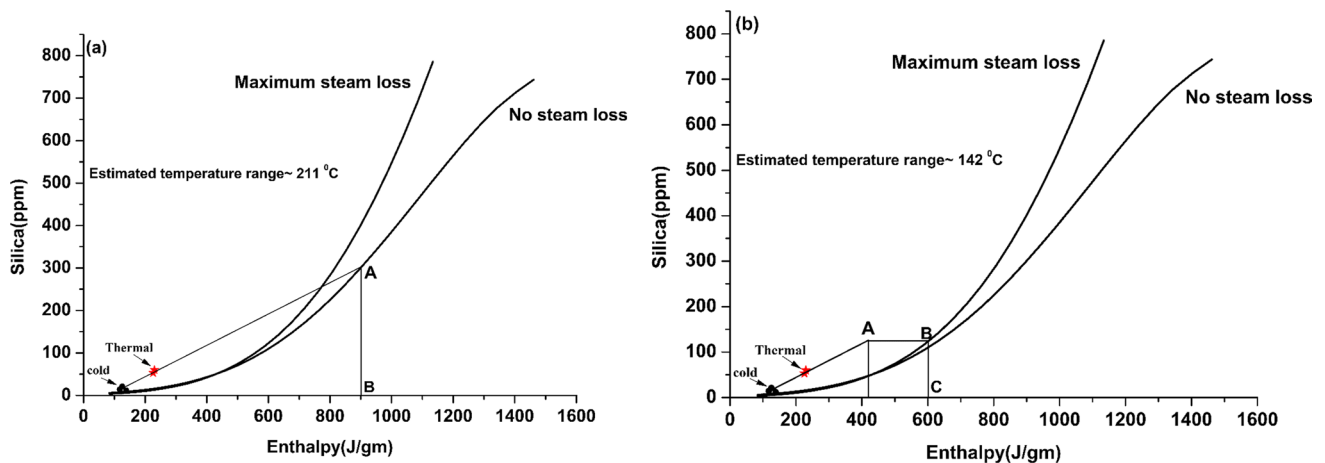


Fig. 9 Enthalpy–silica mixing model for Gujarat thermal waters: **a** assuming no steam loss before mixing and **b** assuming steam loss before mixing

the ascending hot water loses steam or heat before mixing with cold water which is considered in the second method (Fig. 9b). In the second method, a vertical line is drawn from the enthalpy value of 419 J/g (corresponding to 100 °C, the boiling point of water) which intersects the mixing line at point A. From point A, a line parallel to the enthalpy axis intersects the maximum steam loss curve at point B. A vertical line from B intersects the enthalpy axis at point C which indicates the reservoir temperature. Applying this method, the average reservoir temperature turns out to be ~142 °C which is in good agreement with the reservoir temperature computed for Dholera thermal water (DH-1) using multi-component geothermometric method.

Enthalpy–chloride mixing model

Enthalpy–chloride mixing model is very useful in defining various subsurface processes (i.e., mixing, boiling, conductive cooling etc.) and provides useful check on geothermometric calculation (Nicholson 1993; Shoedarto et al. 2020; Pan et al. 2021). Figure 10 represents the enthalpy–chloride mixing model for the present study area. Point A represents the enthalpy value of steam which is fixed at 664 Cal/g. Points, such as S_0 , S_1 , S_2 , and S_3 , represent the issuing enthalpy of Lasundra (LS-1), Bhadiyad (BD-1), Dholera (DH-01), and Tuwa (TA-01) thermal springs, respectively. Steam loss lines are represented by the straight lines connecting the points A and S_x . Points, such as P_0 , P_1 , P_2 , and P_3 , represent the calculated enthalpy of the respective thermal springs based on Na–K–Ca geothermometer. The chloride concentration and enthalpy of the non-thermal water is denoted by the point M. From Fig. 10, it is observed that the P_0 , P_1 , and P_3 points lie on the line joining with the point M (composition of non-thermal water). Curves B and C represent the dilution line or

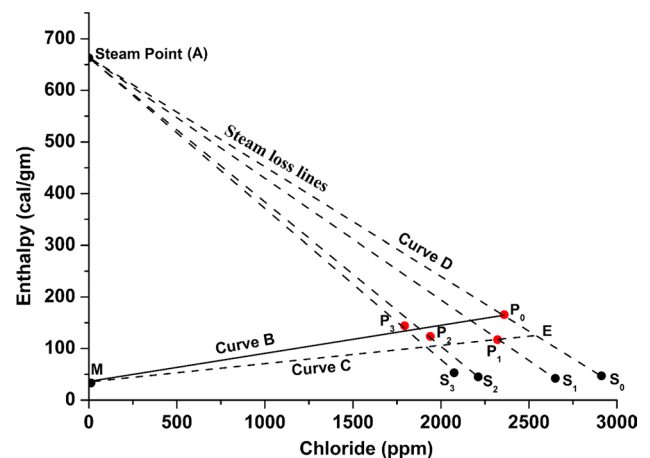


Fig. 10 Enthalpy–chloride mixing model for Gujarat thermal waters

mixing line, whereas curve D represents the upper boundary of boiling curve. The intersection of curve B and curve D at point P_0 gives the upper limit of the enthalpy of the parent fluid which is found to be 164 °C. The upper limit of the reservoir temperature from the enthalpy–chloride mixing model lies within the temperature range deduced from the multicomponent geothermometry method for Lasundra (LS-1), Tuwa (TA-3), and Tulshishaym (TS-1) thermal waters. On the other hand, the intersection of curve C and curve D at the point E provides the lower limit of the enthalpy of the parent fluid which turns out to be 126 °C (after converting enthalpy to temperature) and corroborates well with the reservoir temperature obtained for the Dholera (DH-1) thermal water using multicomponent geothermometry method. Therefore, this enthalpy–chloride mixing model is found to give same range of reservoir temperature as obtained from the multicomponent geothermometry method.

Conclusion

Subsurface temperature estimation in most of the medium/low enthalpy geothermal fields is challenging due to the non-attainment of fluid–rock equilibrium resulting discordant temperature values obtained from different chemical geothermometers. Chemical geothermometers which are based on the assumed chemical equilibrium between thermal water and specific mineral assemblages suffer drawbacks due to the presence of secondary processes, such as mixing/dilution, degassing, etc. during the ascent of thermal waters towards the surface. A similar scenario is encountered in the present study area, which also falls in the medium enthalpy geothermal system. The temperature range estimated from the quartz geothermometer varies from 34 to 105 °C with few of them falling below the surface discharge temperature of the thermal waters, thereby negating the applicability of silica geothermometers. The similar situation happens when K–Mg and Mg–Li geothermometers are applied to estimate the reservoir temperature suggesting interaction with the non-thermal waters near the surface (Mg incorporation). Based on the Giggenbach's (1988) Na–K–Mg triangular diagram, it is observed that although Na–K geothermometer is found to be suitable to estimate the reservoir temperature in Lasundra and Tuwa region, still it provides somewhat higher estimation of reservoir temperature (~ 170 to 226 °C). On the other hand, Na–K–Ca geothermometer provides conservative estimation of subsurface reservoir temperature and in case of thermal waters from Lasundra (LS-1, 2), Tuwa (TA-1, 2, 3, 4, 5), and Tulsishyam (TS-1) region. The estimated subsurface temperature from Na–K–Ca geothermometer ranges from 158 to 175 °C. The multicomponent fluid geothermometry approach resolves this apparent contradiction in estimation of reservoir temperature. The GeoT modelling of the reconstructed fluids (corrected for dilution) at Dholera region (DH-1) provides subsurface temperature in the range of 138 ± 7 °C which matches closely with the values obtained from Na–K–Ca geothermometer (120–126 °C) as well as Na–K geothermometer (131–136 °C) (Giggenbach 1988). In case of thermal waters from Lasundra, Tuwa, and Tulsishyam region, the GeoT modelling results give concordant estimation of reservoir temperature in the range of $\sim 165 \pm 10$ °C. The application of two mixing models, such as enthalpy–silica and enthalpy–chloride mixing models, also give similar estimation of the reservoir temperature as obtained from the multicomponent geothermometry technique. This multicomponent modelling results thus essentially indicate the existence of separate geothermal reservoirs feeding the thermal springs in this region. One reservoir has comparatively lower temperature (~ 130 to 140 °C) and is feeding

thermal springs like Dholera, Maktupur, Bhadiyad, etc., whereas the other reservoir has higher subsurface temperature ($\sim 165 \pm 10$ °C) and is feeding thermal springs in Lasundra, Tuwa, and Tulsishyam regions. Therefore, from the above discussions, it is quite evident that the multicomponent geothermometry is the only viable alternative in providing the correct estimation of subsurface temperature which has also been observed in other medium enthalpy geothermal systems (Battistel et al. 2014; Chatterjee et al. 2017, 2019; Nitschke et al. 2017).

Supplementary Information The online version contains supplementary material available at <https://doi.org/10.1007/s12665-023-11241-2>.

Acknowledgements The authors wish to thank Dr. P. K. Mohapatra, AD, RC&I group, and the officers of GSI associated with this study for their active support and encouragement during the course of the investigation.

Author contributions SC: conceptualization, investigation, methodology, data curation, and draft writing. PM: investigation, sampling, and methodology. TK: supervision, reviewing, and editing manuscript. HJP: project administration and supervision.

Funding The authors have not disclosed any funding.

Data availability All the data is given in this article.

Declarations

Competing interests The authors declare no competing interests.

References

- APHA (American Public Health Association) (1995) Standard methods for the examination of water and wastewater, 19th edn. American Public Health Association, Washington, DC, pp 4–122
- Arnórsson S (1983) Chemical equilibria in Icelandic geothermal systems-implications for chemical geothermometry investigations. *Geothermics* 12:119–128
- Arnórsson S (2000) Isotopic and chemical techniques in geothermal exploration, development and use. International Atomic Energy Agency, Vienna, pp 154–170
- Arnórsson S, Andrésdóttir A (1995) Processes controlling the distribution of boron and chlorine in natural waters in Iceland. *Geochim Cosmochim Acta* 59:4125–4146. [https://doi.org/10.1016/0016-7037\(95\)00278-8](https://doi.org/10.1016/0016-7037(95)00278-8)
- Arnórsson S, Gunnlaugsson E (1985) New gas geothermometers for geothermal exploration-Calibration and application. *Geochim Cosmochim Acta* 49:1307–1325
- Battistel M, Hurwitz S, Evans W, Barbieri M (2014) Multicomponent geothermometry applied to a medium-low enthalpy carbonate-evaporite geothermal reservoir. *Energy Procedia* 59:359–365
- Byrne DJ, Broadley MW, Halldórsson SA et al (2021) The use of noble gas isotopes to trace subsurface boiling temperatures in Icelandic geothermal systems. *Earth Planet Sci Lett* 560:116805
- Chatterjee S, Sinha UK, Deodhar AS, Ansari MA, Singh N, Srivastava AK, Aggarwal RK, Dash A (2017) Isotope-geochemical characterization and geothermometrical modeling of Uttarakhand geothermal field, India. *Environ Earth Sci* 76:638. <https://doi.org/10.1007/s12665-017-6973-2>

- Chatterjee S, Sinha UK, Biswal BP, Jaryal A, Patbhaje S, Dash A (2019) Multicomponent versus classical geothermometry: applicability of both geothermometers in a medium-enthalpy geothermal system in India. *Aquat Geochem* 25:91–108. <https://doi.org/10.1007/s10498-019-09355-w>
- Chatterjee S, Mishra P, Sasi Bhushan K, Goswami P, Sinha UK (2023) Unraveling the paleo-marine signature in saline thermal waters of Cambay rift basin, Western India: Insights from geochemistry and multi isotopic (B, O and H) analysis. *Mar Pollut Bull* 192:115003. <https://doi.org/10.1016/j.marpolbul.2023.115003>
- Chiodini G, Marini L (1998) Hydrothermal gas equilibria: the H₂O–H₂–CO₂–CO–CH₄ system. *Geochim Cosmochim Acta* 62:2673–2687. [https://doi.org/10.1016/S0016-7037\(98\)00181-1](https://doi.org/10.1016/S0016-7037(98)00181-1)
- Fernandez-Turiel J, Llorens J, Lopez-Vera F, Gomez-Artola C, Morell I, Gimeno D (2000) Strategy for water analysis using ICP-MS. *Fresenius J Anal Chem* 368:601–606. <https://doi.org/10.1007/s002160000552>
- Fournier RO (1977) Chemical geothermometers and mixing models for geothermal systems. *Geothermics* 5:40–41
- Fournier RO (1989) The solubility of silica in hydrothermal solutions: practical applications. In: Lectures on geochemical interpretation of hydrothermal water. UNU geothermal training programme, report 10, Reykjavik, Iceland
- Fournier RO (1979a) A revised equation for Na/K geothermometer. *Geotherm Resour Council Trans* 3:221–224
- Fournier RO (1979b) Geochemical and hydrologic considerations and the use of enthalpy-chloride diagrams in the prediction of underground conditions in hot-spring systems. *J Volcanol Geotherm Res* 5:1–16
- Fournier RO, Truesdell AH (1973) An empirical Na–K–Ca geothermometer from natural waters. *Geochim Cosmochim Acta* 37:1255–1275
- Giggenbach WF (1980) Geothermal gas equilibria. *Geochim Cosmochim Acta* 44:2021–2032. [https://doi.org/10.1016/0016-7037\(80\)90200-8](https://doi.org/10.1016/0016-7037(80)90200-8)
- Giggenbach WF (1988) Geothermal solute equilibria. Derivation of Na–K–Mg–K geothermometers. *Geochim Cosmochim Acta* 52:2749–2765
- Giggenbach WF (1995) Variations in the chemical and isotopic composition of fluids discharged from the Taupo Volcanic Zone, New Zealand. *J Volcanol Geotherm Res* 68:89–116. [https://doi.org/10.1016/0377-0273\(95\)00009-J](https://doi.org/10.1016/0377-0273(95)00009-J)
- Goff F, Shevenell L, Gardner JN, Vuataz FD, Grigsby CO (1988) The hydrothermal outflow plume of Valles caldera, New Mexico, and a comparison with other outflow plumes. *J Geophys Res* 93:6041–6058. <https://doi.org/10.1029/JB093iB06p06041>
- GSI (Geological Survey of India) (2001) Geology and mineral resources of Gujarat, Daman and Diu. *Geol. Surv. Ind. Spl. Pub., No. 30 (XIV)*, pp 1–111
- GSI (Geological Survey of India) (2017) Geology and mineral resources of Gujarat, Daman and Diu. *Geol. Surv. Ind. Spl. Pub., No. 30 (Part 14)*, pp 1–137
- Gupta SK, Deshpande RD (2003) Origin of groundwater helium and temperature anomalies in the Cambay region of Gujarat, India. *Chem Geol* 198:33–46. [https://doi.org/10.1016/S0009-2541\(02\)00422-9](https://doi.org/10.1016/S0009-2541(02)00422-9)
- Hou Z, Xu T, Lia S, Jiang Z, Feng B, Cao Y, Fenga G, Yuan Y, Hu Z (2019) Reconstruction of different original water chemical compositions and estimation of reservoir temperature from mixed geothermal water using the method of integrated multicomponent geothermometry: a case study of the Gonghe Basin, northeastern Tibetan Plateau. *China Appl Geochem* 108:104389. <https://doi.org/10.1016/j.apgeochem.2019.104389>
- Keenan JH, Keyes FG, Hill PG, Moore JG (1969) Steam tables—thermodynamic properties of water including vapour, liquid and solid phases (international edition—metric units). Wiley, New York, p 162
- Keesari T, Sinha UK, Deodhar A, Krishna SH, Ansari A, Mohokar H, Dash A (2016) High fluoride in groundwater of an industrialized area of Eastern India (Odisha): inferences from geochemical and isotopic investigation. *Environ Earth Sci*. <https://doi.org/10.1007/s12665-016-5874-0>
- Keesari T, Chatterjee S, Kumar M, Mohokar H, Sinha UK, Roy A, Pant D, Patbhaje SD (2022) Tracing thermal and non-thermal water circulations in shear zones of Eastern Ghats Mobile Belt zone Eastern India- inferences on sustainability of geothermal resources. *J Hydrol* 612:128172. <https://doi.org/10.1016/j.jhydrol.2022.128172>
- Kharaka YK, Lico MS, Law LM (1982) Chemical geothermometers applied to formation waters, Gulf of Mexico and California Basins (abstract). *Am Ass Petrol Geol Bull* 66:588
- Legros H, Marignac C, Mercadier J, Cuney M, Richard A, Wang RC et al (2016) Detailed paragenesis and Li-mica compositions as recorders of the magmatic-hydrothermal evolution of the Maoping W-Sn deposit (Jiangxi, China). *Lithos* 264:108–124. <https://doi.org/10.1016/j.lithos.2016.08.022>
- Lopez JG, Pirez IS, Fernández-Nieto C, Gonzalez IF (1993) Lithium-bearing hydrothermal alteration phyllosilicates related to Portalet fluorite ore (Pyrenees, Huesca, Spain). *Clay Miner* 28:275–283. <https://doi.org/10.1180/claymin.1993.028.2.08>
- Merh S (1995) Geology of Gujarat. Geological Society of India, Bangalore, p 224
- Minissale A, Chandrasekharam D, Vaselli O, Magro G, Tassi F, Pansini GL, Bhrambahut A (2003) Geochemistry, geothermics and relationship to active tectonics of Gujarat and Rajasthan thermal discharges. *India J Volcanol Geotherm Res* 127(1–2):19–32
- Nicholson K (1993) Geothermal fluids chemistry and exploration techniques. Springer, Berlin, pp 22–23
- Nieva D, Nieva R (1987) Developments in geothermal energy in Mexico, Part 12. A cationic geothermometer for prospecting of geothermal resources. *Heat Recov Syst CHP* 7:243–258
- Nitschke F, Held S, Villalon I, Neumann T, Kohl T (2017) Assessment of performance and parameter sensitivity of multicomponent geothermometry applied to a medium enthalpy geothermal system. *Geotherm Energy* 5:12. <https://doi.org/10.1186/s40517-017-0070-3>
- Nitschke F, Held S, Neumann T, Kohl T (2018) Geochemical characterization of the Villarrica geothermal system, Southern Chile, part II: site-specific re-evaluation of SiO₂ and Na-K solute geothermometers. *Geothermics* 74:217–225. <https://doi.org/10.1016/j.geothermics.2018.03.006>
- Olguín-Martínez MG, Peiffer L, Dobson PF, Spycher N, Inguaggiato C, Wanner C, Hoyos A, Wurl J, Makovsky K, Ruiz-Aguilar D (2022) PyGeoT: a tool to automate mineral selection for multicomponent geothermometry. *Geothermics* 104(7):102467. <https://doi.org/10.1016/j.geothermics.2022.102467>
- Pan S, Kong YL, Wang K, Ren YQ, Pang ZH, Zhang C, Wen DG, Zhang LY, Feng QD, Zhu GL, Wang JY (2021) Magmatic origin of geothermal fluids constrained by geochemical evidence: implications for the heat source in the northeastern Tibetan Plateau. *J Hydrol* 603:126985. <https://doi.org/10.1016/j.jhydrol.2021.126985>
- Pang ZH, Reed MH (1998) Theoretical chemical thermometry on geothermal waters: problems and methods. *Geochim Cosmochim Acta* 62:1083–1091
- Pentecost A, Jones B, Renaut RW (2003) What is a hot spring? *Can J Earth Sci* 40(11):1443–1446. <https://doi.org/10.1139/e03-083>
- Rao GSP, Tewari HC (2005) The seismic structure of the Saurashtra crust in northwest India and its relationship with the Reunion Plume. *Geophys J Int* 160(1):318–330

- Reed MH, Sphycher NF (1984) Calculation of pH and mineral equilibria in hydrothermal waters with application to geothermometry and studies of boiling and dilution. *Geochim Cosmochim Acta* 48:1479–1492
- Shah M, Sircar A, Shaikh N, Patel K, Sharma S, Vaidya D (2019) Comprehensive geochemical/hydrochemical and geo-thermometry analysis of Unai geothermal field, Gujarat, India. *Acta Geochim* 38:145. <https://doi.org/10.1007/s11631-018-0291-6>
- Shah M, Sircar A, Shah V, Dholakia Y (2021) Geochemical and geothermometry study on hot-water springs for understanding prospectivity of low enthalpy reservoirs of Dholera Geothermal field, Gujarat, India. *Solid Earth Sci* 6:297–312. <https://doi.org/10.1016/j.sesci.2021.04.004>
- Shoedarto RM, Tadaa Y, Kashiwaya K, Koikea K, Iskandar I (2020) Specifying recharge zones and mechanisms of the transitional geothermal field through hydrogen and oxygen isotope analyses with consideration of water-rock interaction. *Geothermics* 86:101797. <https://doi.org/10.1016/j.geothermics.2019.101797>
- Singh HK, Thankappan A, Mohite P, Sinha SK, Chandrasekharam D, Chandrasekhar T (2018) Geothermal energy potential of Tulsishyam thermal springs of Gujarat, India. *Arab J Geosci* 11:137. <https://doi.org/10.1007/s12517-018-3501-y>
- Spycher N, Peifer L, Sonnenthal E, Saldi G, Reed MH, Kennedy BM (2014) Integrated multicomponent solute geothermometry. *Geothermics* 51:113–123
- Srikarni C, Das S (1996) Stratigraphy and sedimentation history of Champaner Group, Gujarat. *J Indian Assoc Sedim* 15:93–108
- Tonani F (1980) Some remarks on the application of geochemical techniques in geothermal exploration. In: *Proceedings adv. Eur. Geoth. res., second symp., Strasbourg*, pp 428–443
- Truesdell AH, Fournier RO (1977) Procedure for estimating the temperature of a hot water component in mixed water using a plot of dissolved silica vs. enthalpy. *J Res Geol Surv* 5(1):49–52
- Trumbull RB, Slack JF (2018) Boron isotopes in the continental crust: granites, pegmatites, felsic volcanic rocks, and related ore deposits. In: Marschall H, Foster G (eds), *Boron isotopes. Advances in isotope geochemistry*, pp 249–272. https://doi.org/10.1007/978-3-319-64666-4_10
- Verma SP, Pandarinath K, Santoyo E (2008) SolGeo: a new computer program for solute geothermometers and its application to Mexican geothermal fields. *Geothermics* 37(6):597–621
- Xu T, Hou Z, Jia X, Sphycher N, Jiang Z, Feng B, Na J, Yuan Y (2016) Classical and integrated multicomponent geothermometry at the Tengchong geothermal field, Southwestern China. *Environ Earth Sci* 75:1502. <https://doi.org/10.1007/s12665-016-6298-6>
- Yadav K, Sircar A (2019) Integrated 2D joint inversion models of gravity, magnetic and MT for geothermal potentials: a case study from Gujarat, India. *Model Earth Syst Environ Springer* 5(3):963–983

Publisher's Note Springer Nature remains neutral with regard to jurisdictional claims in published maps and institutional affiliations.

Springer Nature or its licensor (e.g. a society or other partner) holds exclusive rights to this article under a publishing agreement with the author(s) or other rightsholder(s); author self-archiving of the accepted manuscript version of this article is solely governed by the terms of such publishing agreement and applicable law.